Article

Discovery Medicine 2025; 37(200): 2019–2031
https://doi.org/10.24976/Discov.Med.202537200.173

Sanguinarine Inhibits VEGF-Induced Cell Migration and Angiogenesis Through Regulating E-Cadherin and p27 Signal Pathway

Li Ying[1], Wei Li[2], Sa Shen[3], Chongsheng Zhang[1], Yangyang Zhang[1], Xiaotian Zhang[1], Wenan Wang[1,*]

[1]Department of Neurology, Chongming Hospital Affiliated to Shanghai University of Medicine & Health Science, 202150 Shanghai, China
[2]Department of Cardiology, Xinhua Hospital Affiliated to Medical College of Shanghai Jiaotong University, 200092 Shanghai, China
[3]Department of Emergency, Xinhua Hospital Affiliated to Medical College of Shanghai Jiaotong University, 200092 Shanghai, China
*Correspondence: wenan_wang1968@126.com (Wenan Wang)
Submitted: 29 August 2024 Revised: 18 October 2024 Accepted: 23 October 2024 Published: 20 September 2025

Background: Sanguinarine, a benzophenanthridine alkaloid, is extracted from the rhizomes of *Sanguinaria canadensis* and other poppy species (*Fumaria*). Although its antitumor activity is not fully understood, sanguinarine has demonstrated various biological effects, including antioxidant, antimicrobial, and anti-inflammatory properties. This work hypothesizes that sanguinarine's novel anti-angiogenic mechanism may enhance the efficacy of anticancer therapy.

Methods: The Cell Counting Kit-8 (CCK-8) assay and colony formation assay were conducted to evaluate the effect of sanguinarine on angiogenesis. Preliminary mechanisms of sanguinarine were investigated through cell cycle and apoptosis assays. A tube formation assay was performed to examine the impact of sanguinarine on angiogenesis *in vitro*. RT-qPCR and western blot analyses were primarily used to elucidate the underlying mechanisms, which were further validated through a vascular endothelial growth factor (VEGF) recovery experiment. Additionally, an animal xenograft model was employed to assess the effect of sanguinarine on tumor growth and to analyze potential toxicity.

Results: Sanguinarine significantly inhibited the proliferation of rat smooth muscle cells (A7r5) and human microvascular endothelial cells (HMVECs) and increased the cell population in the G2/M phase ($p < 0.05$). Sanguinarine also reduced cell migration capacity and angiogenesis ($p < 0.05$). These effects were mediated by inhibiting the VEGF signaling pathway, as sanguinarine downregulated VEGF expression at both mRNA and protein levels, with partial recovery observed upon VEGF supplementation in the medium ($p < 0.05$). Additionally, sanguinarine exposure inhibited phosphorylation activity across multiple kinases downstream of VEGF ($p < 0.05$). In animal experiments, sanguinarine suppressed tumor growth without significant toxicity ($p < 0.05$).

Conclusion: Sanguinarine exerts an inhibitory effect on blood vessel cell proliferation, presenting a valuable therapeutic approach in cancer treatment.

Keywords: sanguinarine; VEGF; angiogenesis; migration; E-cadherin; p27

Introduction

Cancer remains a leading cause of death worldwide; the rapid proliferation of tumor cells often surpasses the rate of neovascularization, resulting in a hypoxic tumor microenvironment. Tumor angiogenesis supports tumor growth and metastasis, facilitating infiltration into other tissues [1]. Various factors regulate angiogenesis, including platelet-derived growth factor (PDGF) and its receptor (PDGFR), fibroblast growth factor (FGF) and its receptor (FGFR), and vascular endothelial growth factor (VEGF), which contribute to endothelial cell adhesion, maturation, and are involved in cell proliferation, vascular remodeling, and new blood vessel formation [2]. Studies consistently indicate that tumor angiogenesis enhances tumor growth and migration, underscoring the need for further research to identify effective anti-angiogenic therapies [3,4].

Sanguinarine is a quaternary benzophenanthridine alkaloid extracted from roots of the *Sanguinaria canadensis* plant and other medicinal poppy *Fumaria* species [5,6]. Increasing research has focused on its anti-cancer potential; preclinical studies have demonstrated its antioxidant, anti-inflammatory, proapoptotic, and growth inhibitory properties against various cancer cells at micromolar concentrations [7]. Moreover, recent studies indicated that the cytotoxicity of sanguinarine is more pronounced in carcinoma cells than in normal cells [8,9], supporting its potential as a new anticancer-targeted drug. While previous research verified sanguinarine's antiangiogenic effects, the understanding of its precise mechanism and intracellular molecular-

targeted protein remains limited. Therefore, through a series of *in vitro* and *in vivo* experiments, this study aims to investigate the molecular mechanisms of sanguinarine's anti-angiogenic properties.

Pathological angiogenesis is critical in cancer initiation, progression, and metastasis. VEGF binds to its receptors, promoting tumor-associated neovascularization [10]. Recent studies have focused on anti-VEGF agents and inhibition within the VEGF signaling pathway due to their therapeutic potential [11,12]. However, clinical trials have reported severe side effects and tumor recurrence following target therapy [13]. Adjuvant therapies may help address these issues and enhance VEGF-targeted approaches. Sanguinarine has shown promise as an antiangiogenic agent [14,15]; however, there are few studies on the effects of sanguinarine on VEGF and angiogenesis [16,17].

Therefore, investigating and elucidating the underlying mechanisms of sanguinarine-induced angiogenesis inhibition is crucial for developing highly efficacious and specific sanguinarine-based therapeutic agents. This study examines the mechanisms by which sanguinarine affects tumor neovascularization, migration, and invasion, aiming to provide a foundation for developing novel targeted therapies for tumors.

Materials and Methods

Cell Culture

Rat smooth muscle cells (A7r5, CRL-1444), human microvascular endothelial cells (HMVECs, CRL-3243), and MCF-7 cells (HTB-22™) were obtained from the American Type Culture Collection (ATCC, Manassas, VA, USA). A7r5 and MCF-7 cells were cultured in Dulbecco's Modified Eagle Medium (DMEM) (Gibco BRL, Grand Island, NY, USA) with 10% fetal bovine serum (FBS) (Hyclone, Logan, UT, USA) and antibiotics, incubated at 37 °C in 5% CO_2 for 12 hours as previously described. HMVEC cells were cultured in MCDB-131 medium (Gibco BRL, Grand Island, NY, USA), supplemented with 10% fetal calf serum (FCS) (Hyclone, Logan, UT, USA), 10 ng/mL basic fibroblast growth factor (bFGF), and 10 µg/µL heparin (Sigma-Aldrich, St. Louis, MO, USA), and incubated at 37 °C in 5% CO_2 for 12 hours. All cell lines were authenticated by Short Tandem Repeat (STR) identification and underwent mycoplasma testing.

Animal Model

A total of 20 female nude mice (aged 4–6 weeks, 18–22 g) were purchased from the Experimental Animal Center of Shanghai Jiaotong University and housed in a specific pathogen-free (SPF) facility with appropriate temperature and humidity. All animal experiments were conducted in accordance with the guidelines of the Animal Ethics Committee of Medical Discovery Leader (MDL, Approval number: MDL2022-06-14-02) and followed the Guide for the Care and Use of Laboratory Animals published by the Chinese National Institutes of Health.

The tumor model was established by injecting the mice with 1×10^6 MCF-7 cells suspended in 100 µL of Phosphate Buffered Saline (PBS). Seven days after inoculation, tumor-bearing mice (n = 16) with a tumor size of approximately 100 mm^3 were included in further experiments, and mice that did not enter further experiments were euthanized. The mice were randomly divided into control and treatment groups. Mice in the treatment group received 10 mg/kg sanguinarine (n = 8) while the control group received PBS, both administered intravenously twice a week for six weeks. Throughout the experiment, the physiological status of the mice was monitored.

After 6 hours of fasting, the mice were euthanized by cervical dislocation, and the tumors were rapidly excised. Tumor volume and weight were measured. Additionally, the main organs (heart, liver, kidney, and lung) were dissected and fixed in 4% polyoxymethylene for hematoxylin and eosin (HE) staining.

HE Staining

A HE staining kit (Beyotime, cat: C0105, Shanghai, China) was used to analyze the morphological changes in the main organs of mice following sanguinarine treatment. All procedures adhered to the manufacturer's instructions. The main organs (heart, kidney, liver, and lung) were embedded in paraffin and sectioned. The paraffin sections were deparaffinized, hydrated, and stained with hematoxylin staining solution for 5–20 minutes, followed by treatment with a differentiation solution for 30 seconds. The sections were then placed in eosin dye solution, washed, soaked in distilled water, dehydrated with alcohol, and cleared with xylene. Finally, the sections were mounted on slides, sealed with neutral gum, and observed under a microscope (Leica DM3000, Leica, Wetzlar, Germany) at 400× magnification.

Tube-Formation Assay

The tube formation assay was employed to assess angiogenesis *in vitro*. A total of 1×10^4 A7r5 and HMVEC cells were seeded in 24-well plates pre-coated with Matrigel (Corning, Corning, NY, USA) and cultured in medium supplemented with 50 ng/mL VEGF (R&D Systems, Minneapolis, MN, USA). After 24 hours, images were captured under a microscope, and the branching points were quantified using ImageJ software (Image-Pro Plus 6.0, NIH, Bethesda, MD, USA).

Reagents

Sanguinarine chloride (Sigma-Aldrich, USA) was dissolved in Dimethyl sulfoxide (DMSO) and stored at –20 °C. Recombinant human VEGF was purchased from R&D Systems (Minneapolis, MN, USA).

Cell Counting Kit-8 (CCK-8) Assay

The CCK-8 kit (Beyotime, China) was utilized to assess the anti-proliferation effect of sanguinarine following standard protocols. A total of 5 $\times$ 10^3 cells were seeded into a 96-well plate and allowed to adhere overnight. The cells were then stimulated with a series of sanguinarine dilutions (0.5 µM, 1 µM, 2 µM, 4 µM, and 6 µM) for 24, 48, and 72 hours. Following treatment, 10 µL of CCK-8 was added to each well, and the cells were cultured for an additional 4 hours. Finally, the absorbance was measured at 492 nm using a microplate spectrophotometer (Multiskan, Thermo Scientific, Waltham, MA, USA). Cell survival rate = [(As– Ab)/(Ac – Ab)] $\times$ 100% inhibition rate = [(Ac – As)/(Ac – Ab)] $\times$ 100%; As: absorbance of experimental Wells (containing cells, medium, CCK-8 solution and drug solution); Ac: absorbance of control Wells (containing cells, medium, CCK-8 solution, without drug); Ab: absorbance of blank Wells (containing medium and CCK-8 solution, without cells and drugs).

Clonogenic Assay

Cells were seeded at 300 cells per well in 35 mm plates containing 0.6% agarose. After attachment, a series of sanguinarine dilutions was added to the medium. After 14 days, the cells were stained with crystal violet solution (Sigma-Aldrich, USA), and images of the plates were captured using a camera (Canon PowerShot A640, Canon, Tokyo, Japan). Colonies with $\geq$50 cells were counted.

Cell Cycle Analysis

For cell cycle analysis, cells were treated with a series of sanguinarine dilutions for 24 hours, and cell-cycle distribution was assessed by measuring the DNA content. The cells were stained using propidium iodide (PI)/RNase A staining buffer (Beyotime, Shanghai, China) and evaluated via flow cytometry analysis (BD, Franklin Lakes, NJ, USA).

Apoptosis Analysis

Cells were harvested 48 hours after treatment with a series of sanguinarine dilutions and tested using a Fluorescein Isothiocyanate (FITC)-conjugated Annexin V/PI Apoptosis Detection Kit (Beyotime, Shanghai, China) according to the standard protocols. Cells resuspended at 50 to 100,000 were centrifuged at 1000 g for 5 min, the supernatant was discarded, and 195 µL of Annexin V-FITC binding solution was added to gently resuspend the cells. 5 µL of Annexin V-FITC was added and mixed gently. Ten µL of propidium iodide staining solution was added and gently mixed. The cells were incubated in the dark for 10–20 min at room temperature (20–25 °C) and subsequently placed in an ice bath. Aluminum foil can be used for light protection. Cells can be resuspended 2–3 times during incubation to improve staining. Samples were analyzed by flow cytometry (BD, Franklin Lakes, NJ, USA).

Wounding Healing Assay

Exactly 2.5 $\times$ 10^5 A7r5 and HMVEC cells were seeded onto 0.1% gelatin-coated 6-well plates. Wounds were created in a confluent cell monolayer using a 200-µL sterile pipette tip, followed by washing with PBS. The cells were then treated with sanguinarine (0.5 µM, 1 µM, 2 µM) alone, or with VEGF (30 ng/mL) $\pm$ sanguinarine (1 µM, 2 µM) for 24 hours. Images of the plates were captured under a microscope (Leica, Wetzlar, Germany).

Transwell Assay

A total of 1 $\times$ 10^4 A5r7 and HMVEC cells were seeded in the Transwell inserts with 8-mm pores (BD bioscience, San Jose, CA), and serum-free medium with 2.0 µM sanguinarine were added to the bottom chamber and incubated for 24 hours. Medium without supplementation of sanguinarine was used as a control. Cells on the upper side were wiped off, and cells on the lower surface were stained with crystal violet solution. Cells were counted in four random fields using a microscope (Leica, Wetzlar, Germany).

Assay of VEGF Secretion

Further, 1 $\times$ 10^5 A7r5 and HMVEC cells were cultured in normal medium in 12-well plates for 24 hours. Afterward, the cells were treated with a low-serum medium containing different concentrations of sanguinarine for an additional 12 hours. The VEGF concentrations in the supernatant were analyzed using a quantitative Enzyme-linked Immunosorbent Assay (ELISA) kit (R&D Systems, Minneapolis, MN, USA) according to the manufacturer's protocol. The absorbance values were measured at 539 nm using a microplate spectrophotometer (Multiskan, Thermo Scientific, Waltham, MA, USA).

Reverse Transcription-Polymerase Chain Reaction (RT-PCR)

Total RNAs were isolated using a Trizol reagent (Invitrogen, Carlsbad, CA, USA) and subsequently converted to cDNA using M-MLV reverse transcriptase and Oligo-dT primers. RT-qPCR analysis was performed using the ABI 7700 sequence detector (Applied Biosystems, Foster City, CA, USA) along with a matching SYBR nucleic acid staining kit (Takara, Otsu, Japan). The sequences of the primers used are as follows: *VEGF*: Forward: 5′-AGGGCAGAATCATCACGAAGT-3′, Reverse: 5′-AGGGTCTCGATTGGATGGCA-3′; *p27*: Forward: 5′-CGGCTCATGGGCGACTATC-3′, Reverse: 5′-TGTCTTGGAGGAGGATCGTCC-3′; *Cyclin A*: Forward: 5′-GAGGTCCCGATGCTTGTCAG-3′, Reverse: 5′-GTTAGCAGCCCTAGCACTGTC-3′; *Cdc2*: Forward: 5′-AAACTACAGGTCAAGTGGTAGCC-3′, Reverse: 5′-TCCTGCATAAGCACATCCTGA-3′; *E-cadherin*: Forward: 5′-CCTGACTGTGGAGGCCAAAGA-3′, Reverse:

5′-TTCTCACACACTTTGGGCTGGTAG-3′; *Vimentin*: Forward: 5′-GACGCCATCAACACCGAGTT-3′, Reverse: 5′-CTTTGTCGTTGGTTAGCTGGT-3′; *Slug*: Forward: 5′-TGTGACAAGGAATATGTGAGCC-3′, Reverse: 5′-TGAGCCCTCAGATTTGACCTG-3′; *Actin*: Forward: 5′-CACCATCGCCAGGACCAT-3′, Reverse: 5′-GAACTCCTCGGGACCCAG-3′.

The qPCR primers for rats are as follows: *VEGF*: Forward: 5′-GTCATCCCTCCCACACAGTG-3′, Reverse: 5′-CTTCATCATTGCAGCAGCCC-3′; *p27*: Forward: 5′-GTCTCAGGCAAACTCTGAG-3′, Reverse: 5′-GTTTACGTCTGGCGTCGAAG-3′; *Cyclin A*: Forward: 5′-GTCAACCCCGAAAAAGTGGC-3′, Reverse: 5′-CCGAGTCTTGAGCCTCTGC-3′; *Cdc2*: Forward: 5′ATGGATTCTTCGCTCGTT-3′, Reverse: 5′-TCTGCCAGTTTGATTGTTC-3′; *E-cadherin*: Forward: 5′-CCCCTGTTGGCGTTTTCATC-3′, Reverse: 5′-ACTTGTCAATGGCTTCTCTGT-3′; *Vimentin*: Forward: 5′-AATGACCGCTTCGCCAACTA-3′, Reverse: 5′-CGCAACTCCCTCATCTCCTC-3′; *Slug*: Forward: 5′-GCCTTTCTCTTGCCCTCACT-3′, Reverse: 5′-ACACAGCAGCCAGATTCCTC-3′; *Actin*: Forward: 5′-TCTGTGTGGATTGGTGGCTC-3′, Reverse: 5′-CGGACTCATCGTACTCCTGC-3′.

Relative gene expression was normalized using endogenous actin as a reference, following the $2^{-\Delta\Delta Ct}$ method.

Western Blotting

Cells were lysed in Radio Immunoprecipitation Assay (RIPA) buffer, and the protein concentration was quantified using the Pierce Bicinchoninic Acid Assay (BCA) reagent (Thermo Scientific). Proteins were electrophoretically separated on a 10–15% Sodium Dodecyl Sulfate Polyacrylamide Gel Electrophoresis (SDS-PAGE) gel and subsequently transferred onto a nitrocellulose membrane. The membrane was blocked with 5% skimmed milk to prevent nonspecific binding. Following this, the membrane was incubated overnight at 4 °C with a series of primary antibodies purchased from Abcam (Waltham, MA, USA), diluted to 1:2000. The antibodies used included p27 (ab32034), Cyclin A (ab32386), Slug (ab302780), Cdc2 (ab32444), Vimentin (ab92547), E-cadherin (ab40772), c-Jun N-terminal Kinase (JNK) (ab110724), Phospho-c-Jun N-terminal Kinase (pJNK) (ab76572), Phospho-Protein Kinase B (pAKT) (ab38449), Protein Kinase B (AKT) (ab8805), Phospho-p38 Mitogen-activated Protein Kinase (pp38) (ab4822), p38 Mitogen-activated Protein Kinase (p38) (ab170099), Phospho-Focal Adhesion Kinase (pFAK) (ab81298), Focal Adhesion Kinase (FAK) (ab40794), Phospho-Phosphatidylinositol 3-Kinase (pPI3K) (ab151549), Phosphatidylinositol 3-Kinase (PI3K) (ab283852), and β-actin (ab8226). After the primary antibody incubation, membranes were probed with anti-mouse (ab6728) or anti-rabbit (ab6721) secondary antibodies. Protein bands of interest were visualized using the enhanced chemiluminescence detection system (GE, Fairfield, CO, USA) and quantified using ImageJ software.

Statistical Analysis

The quantitative data were presented as mean ± Standard Deviation (SD) unless otherwise specified. Statistically significant differences were calculated using SPSS software (version 23.0, IBM SPSS Statistics, Chicago, IL, USA). For comparisons between two groups, Student's *t*-test was employed, while one-way analysis of variance (ANOVA) followed by the post hoc Tukey test was used for comparisons among multiple groups. A *p*-value of less than 0.05 was considered indicative of a significant difference. ImageJ software (Image-Pro Plus 6.0, NIH, Bethesda, MD, USA) was used to analyze and process the images.

Results

Sanguinarine Inhibits Vascular Smooth Muscle Cell Proliferation, Colony Formation and Increases the Population of Cells at the G2/M Phase

The structural characterization of sanguinarine is illustrated in Fig. 1A. The cytotoxic activity of sanguinarine against rat smooth muscle cells (A7r5) and HMVEC cells were evaluated using CCK-8 assays to determine whether sanguinarine exposure influenced the proliferation of these blood vessel constituent cells. Upon exposure to sanguinarine at concentrations of 0.5, 1.0, 2.0, 4.0, and 6.0 µM for 24 hours, we observed a cell viability reduction of 5%, 10%, 24%, 45%, and 56% for A7r5 cells, and 7%, 21%, 36%, 50%, and 59% for HMVEC cells, respectively. This inhibitory effect was statistically significant at all tested doses (Fig. 1B, $p < 0.05$). The Half Maximal Inhibitory Concentration (IC50) values at 48 hours for A7r5 and HMVEC cells were calculated to be approximately 3 µM and 2.5 µM, respectively. Consequently, 2 µM sanguinarine was selected as the working solution for subsequent experiments. These findings indicate that even low concentrations of sanguinarine significantly interfere with cell proliferation.

The results of the colony formation, cell cycle, and apoptosis assays demonstrated that sanguinarine caused a modest decrease in the number of colonies formed at 1 µM, with a significant reduction observed at 2 µM (Fig. 1C, $p < 0.05$). To explore the potential effects of sanguinarine on the cell cycle and apoptosis, A7r5 and HMVEC cells were exposed to the indicated doses of sanguinarine or vehicle for 24 hours. The cell cycle distribution of A7r5 and HMVEC cell lines was analyzed before and after sanguinarine treatment. Compared to the control group, sanguinarine treatment resulted in an arrest in the G2/M phase, with the population of G2/M cells increasing in a concentration-dependent manner (Fig. 1D, $p < 0.05$). Conversely, no significant pro-apoptotic effect of sanguinarine was observed in either A7r5 or HMVEC cells (Fig. 1E). Collectively,

these findings suggest that sanguinarine-mediated inhibition of cell proliferation is likely associated with cell cycle arrest in a concentration-dependent manner.

Sanguinarine Inhibits Cell Migration in Vascular Smooth Muscle Cells and Microvascular Endothelial Cells

Scratch wound and Transwell assays were conducted on A7r5 and HMVEC cells to further elucidate the effect of sanguinarine on endothelial cell migration. The wound healing experiments demonstrated that sanguinarine significantly inhibited cell migration (Fig. 2A, $p < 0.05$). In alignment with these findings, Transwell assays revealed that sanguinarine treatment resulted in a 2- to 3-fold reduction in the penetration of A7r5 and HMVEC cells (Fig. 2B, $p < 0.05$). These results indicate that sanguinarine significantly suppresses the invasion of A7r5 and HMVEC cells while exhibiting no notable toxic effects.

Sanguinarine Up-Regulates p27 and E-Cadherin

To investigate the molecular mechanism underlying the action of sanguinarine, RT-qPCR and western blot analyses were performed to assess the regulatory profile associated with cell cycle regulation and migration. Notably, p27 and E-cadherin exhibited significant upregulation in response to sanguinarine exposure, both at the mRNA and protein levels, while Cyclin A, Cdc2, Vimentin, and Slug showed no such changes (Fig. 3). Given that VEGF plays a crucial role in physiological and pathological neovascularization, we hypothesized that the observed upregulation of p27 and E-cadherin expression following sanguinarine treatment may be linked to the downregulation of VEGF expression.

Sanguinarine Inhibits Cell Proliferation, Migration, and Vessel Formation by Downregulating VEGF Expression

Given that VEGF is a crucial target in our study, we first aimed to determine whether sanguinarine treatment could inhibit its expression using qPCR analysis (Fig. 4A,B, $p < 0.05$). Our findings indicated that sanguinarine significantly inhibited VEGF expression in a dose- and time-dependent manner. Specifically, when A7r5 and HMVEC cell were treated with 2 μM sanguinarine for 24 hours, there was approximately a 40% reduction in VEGF secretion compared to untreated cells. Consistent with these observations, similar trends were observed in VEGF secretion when measured using ELISA (Fig. 4C,D, $p < 0.05$).

To further elucidate the relationship between sanguinarine and VEGF, we treated A7r5 and HMVEC cells with 2 μM sanguinarine in the presence of 10 ng/mL VEGF for 24 hours and conducted CCK-8 assays, cell cycle analysis, and scratch wound assays (Fig. 4E–G, **Supplementary Fig. 1**, $p < 0.05$). The results demonstrated that the anti-proliferative effects of sanguinarine could be partially reversed by VEGF treatment, which also attenuated the inhibition of cell migration induced by sanguinarine in both A7r5 and HMVEC cells.

Additionally, to assess the antiangiogenic potential of sanguinarine, we performed *in vitro* tube formation assays. The findings confirmed that sanguinarine effectively suppressed angiogenesis in A7r5 and HMVEC cells (Fig. 4H, $p < 0.05$). Collectively, these results suggest that sanguinarine inhibits cell proliferation, migration, and tube formation capacity primarily by downregulating VEGF expression.

Sanguinarine Inhibits VEGF-Mediated Protein Expression

A series of protein levels and phosphorylation states were analyzed to investigate the changes in intercellular signaling in response to the reduction of VEGF induced by sanguinarine. Preliminary results indicated that sanguinarine treatment led to significant dephosphorylation of key signaling proteins, including JNK, Akt (Ser473), p38 (Tyr182), FAK (Tyr397), and PI3K (Fig. 5 and **Supplementary Fig. 2**). However, the aforementioned phosphorylation inactivation was significantly or completely reversed when 10 ng/mL VEGF was added to the medium system (Fig. 5). The observed dephosphorylation of these proteins was associated with enhanced regulation of the cell cycle and an upregulation of p27 and E-cadherin expression, leading to cell cycle arrest. RT-qPCR showed no significant mRNA changes, indicating post-transcriptional regulation (**Supplementary Fig. 3**) Collectively, these findings suggest that sanguinarine disrupts cell dynamics through the modulation of VEGF and its downstream signaling pathways.

Sanguinarine Inhibits the Tumor Growth In Vivo and Toxicity Evaluation

A subcutaneous nude mouse model was established to validate the effects of sanguinarine on tumor growth *in vivo*. Tumor weight and volume measurements revealed that sanguinarine significantly inhibits tumor growth compared to the controls (Fig. 6A, $p < 0.01$). Additionally, histological examination of HE-stained tissue specimens from the heart, liver, lung, and kidney of the mice showed no significant differences in the structure of both nuclear and cytoplasmic components after sanguinarine treatment, confirming its non-toxic nature. Throughout the experiment, no adverse effects of sanguinarine on the mice were observed (Fig. 6B). In summary, the *in vivo* toxicity tests indicate that sanguinarine effectively inhibits tumor growth without remarkable toxic side effects.

Discussion

Most solid tumors rely on angiogenesis, a process orchestrated by various activators and inhibitors, where VEGF and its receptors play crucial roles as rate-limiting

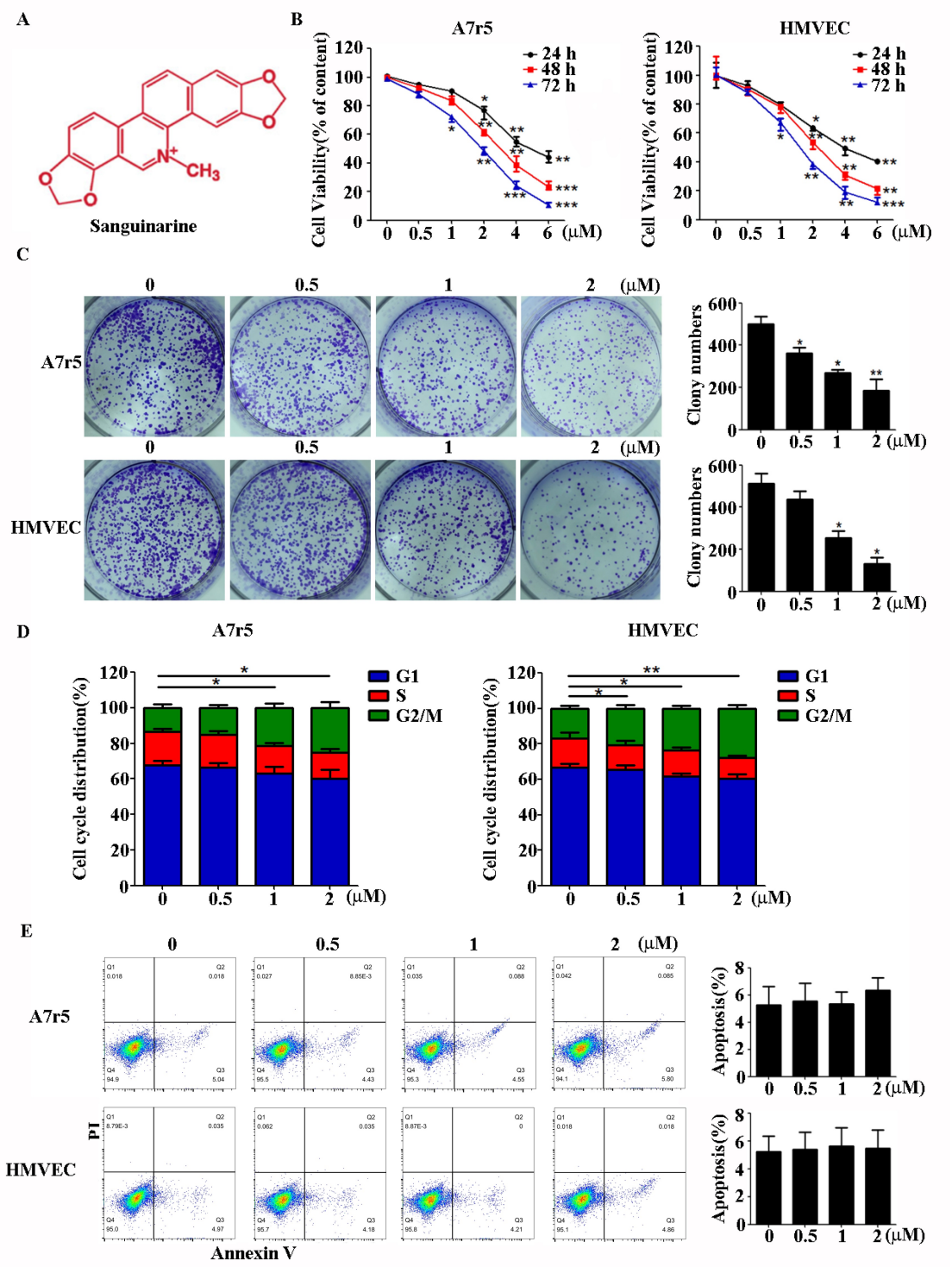

Fig. 1. Sanguinarine inhibited vascular smooth muscle cell proliferation, colony formation and increased population of cells at G2/M phase. (A) Structural characterization of sanguinarine. (B) Rat smooth muscle cells (A7r5) and human microvascular endothelial cells (HMVECs) were treated with a series of sanguinarine dilutions (0.5 μM; 1 μM; 2 μM; 4 μM; 6 μM) for 24 hours, 48 hours and 72 hours. Cell viability was assessed using the Cell Counting Kit-8 (CCK-8) assay. (C) Soft-agar colony formation assays were performed on A7r5 and HMVEC cells exposed to sanguinarine at concentrations of 0.5 μM, 1 μM, and 2 μM, compared to untreated controls. The histograms on the right present the statistical results of the colony counts. (D) Cell-cycle distribution of A7r5 and HMVEC cells stimulated with 0.5 μM, 1 μM, and 2 μM sanguinarine, assessed by flow cytometry. (E) The analysis of cell apoptosis in A7r5 and HMVEC cells exposed to 0.5 μM, 1 μM, and 2 μM sanguinarine, also conducted using flow cytometry. The histograms on the right display the statistical results of the apoptosis rates (%). n = 3. *$p < 0.05$, **$p < 0.01$, and ***$p < 0.001$ compared to 0 μM.

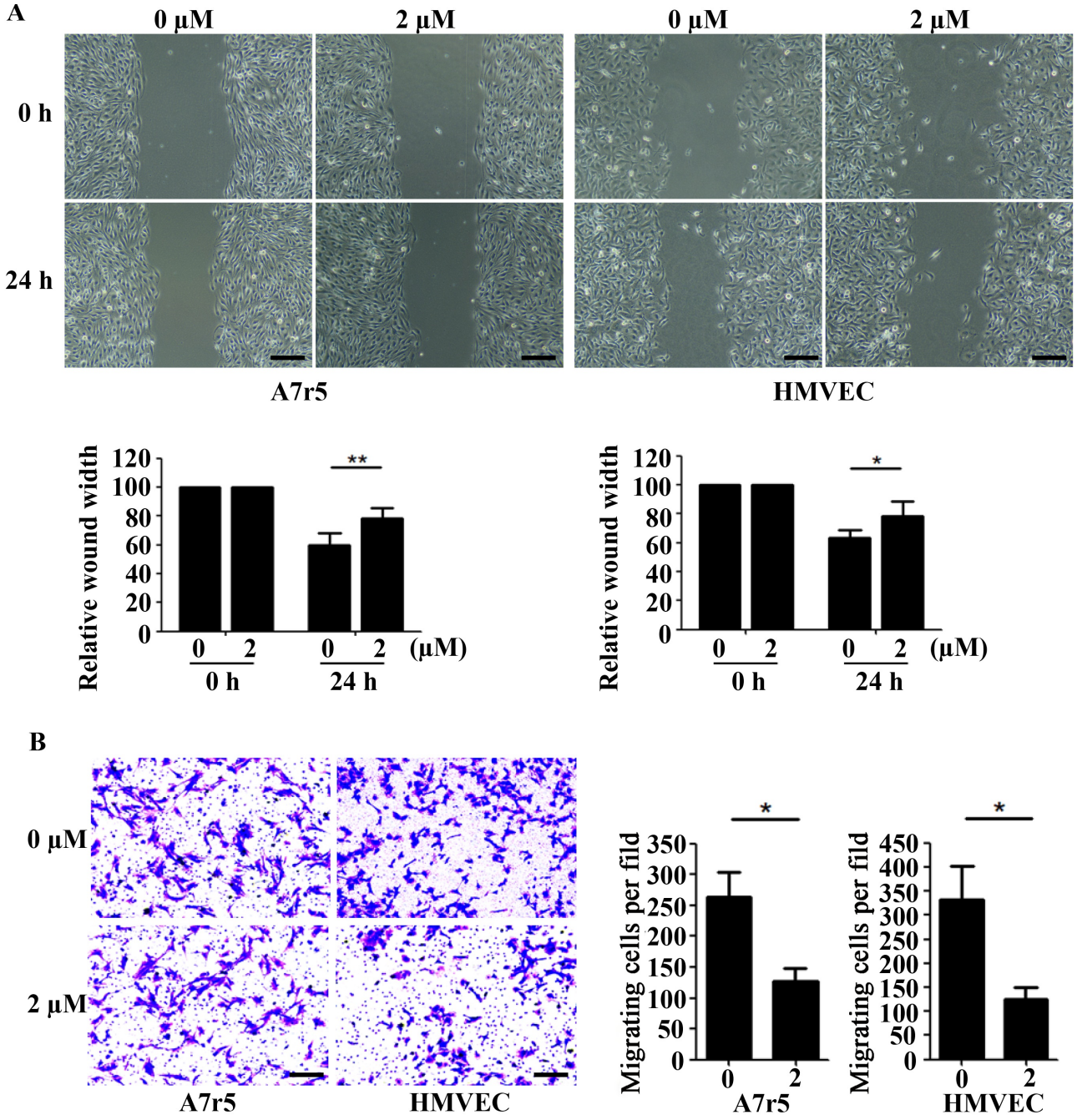

Fig. 2. Sanguinarine inhibited cell migration in vascular Smooth Muscle cells and microvascular endothelial cells. (A) The ability of cell migration of A7r5 and HMVEC cells exposed with 2 μM sanguinarine or not were assessed by wounding healing assay. Histograms on the lower were statistical results of scratch pitch. Scale bar = 50 μm. (B) The left pictures were results of crystal violet staining of A7r5 and HMVEC cells exposed with 2 μM sanguinarine or not. Histograms on the right were the number of invasion cells. Scale bar = 20 μm. n = 3. *$p < 0.05$ compared to 0 μM.

molecules. Research indicates that VEGF exerts a powerful influence on both physiological and pathological angiogenesis by binding to its tyrosine kinase receptors and activating various downstream signaling proteins [18]. Previous studies have confirmed that sanguinarine possesses potent anticancer activity against a variety of tumors [7,8]; however, there is a paucity of research addressing its anti-angiogenic effects. This study aimed to elucidate the underlying mechanism by which sanguinarine regulates angiogenesis.

In this work, sanguinarine at micromolar concentrations significantly inhibited vascular endothelial cell proliferation, colony formation, and vessel formation, while also inducing cell cycle arrest and disrupting cell migra-

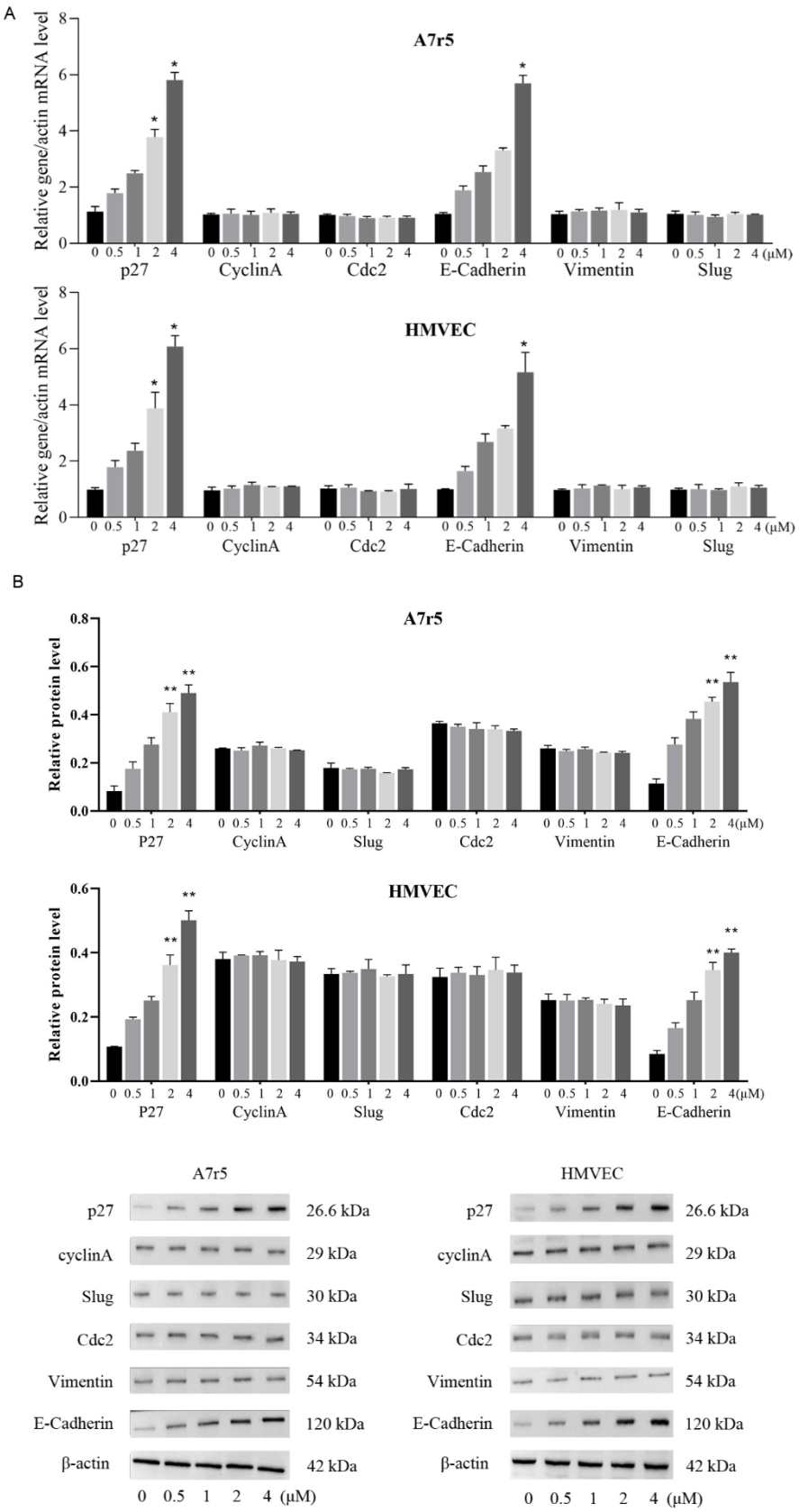

Fig. 3. Sanguinarine up-regulated p27 and E-cadherin. (A,B) A7r5 and HMVEC cells were treated with 0.5 μM, 1 μM, 2 μM and 4 μM sanguinarine, respectively, for 24 hours. RT-qPCR (A) and western blot (B) were used to detect p27, Cyclin A, Cdc2, E-cadherin, Vimentin and Slug expression. n = 3. *$p < 0.05$, **$p < 0.01$, vs compared to 0 μM.

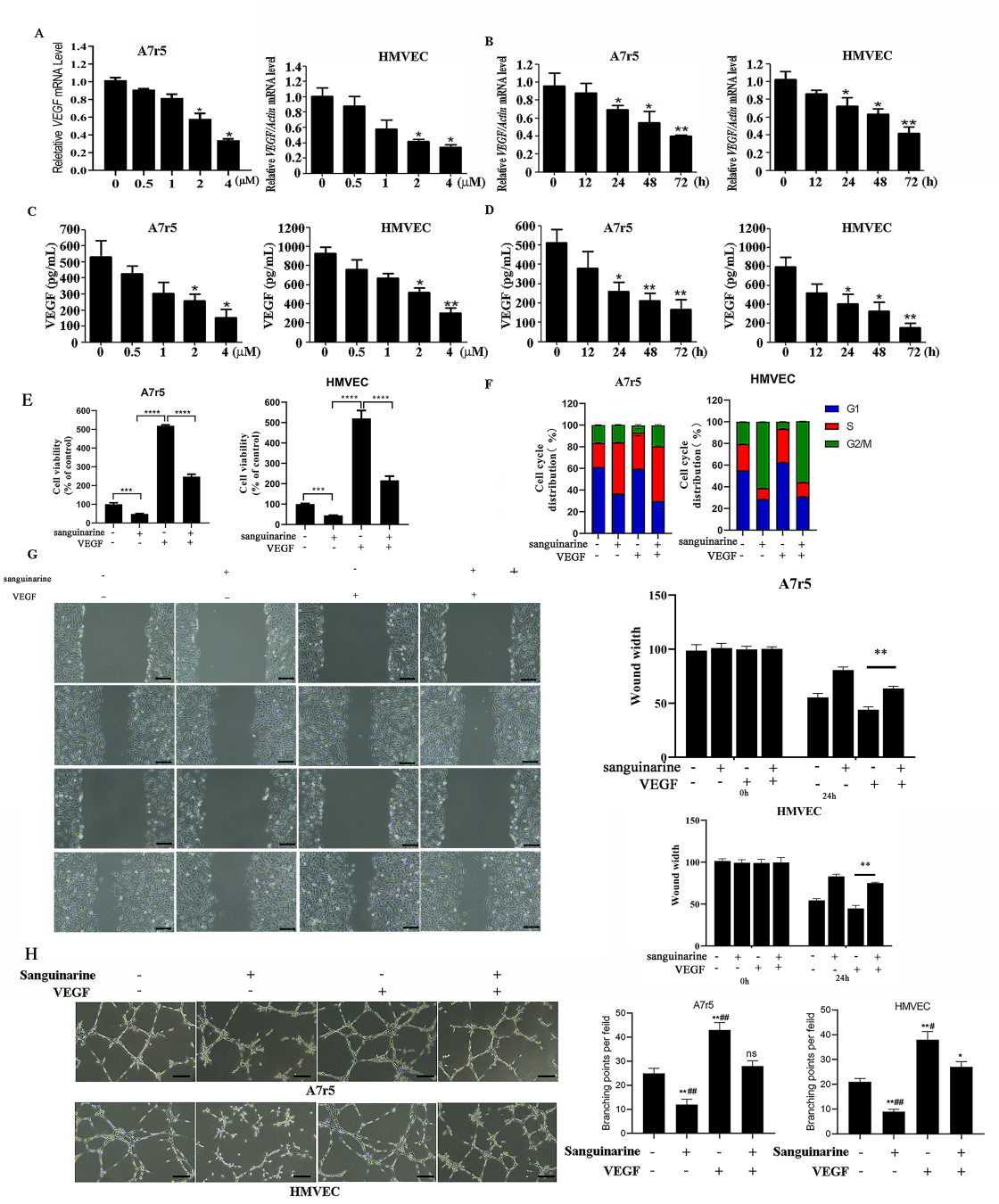

Fig. 4. Sanguinarine inhibited cell proliferation and migration through inhibition of vascular endothelial growth factor (VEGF) expression. (A) A7r5 and HMVEC cells were treated with varying concentrations of sanguinarine (0.5 μM, 1 μM, 2 μM, and 4 μM) for 24 hours, after which the mRNA levels of VEGF were quantified using RT-qPCR. (B) In another experiment, A7r5 and HMVEC cells were exposed to 2 μM sanguinarine for different time points (12 hours, 24 hours, 48 hours, and 72 hours), and the mRNA levels of VEGF were again assessed by RT-qPCR. (C) Additionally, the levels of VEGF secretion were measured using Enzyme-linked Immunosorbent Assay (ELISA) following treatment with 0.5 μM, 1 μM, 2 μM, and 4 μM sanguinarine for 24 hours in A7r5 and HMVEC cells. (D) The VEGF secretion levels were also evaluated in cells treated with 2 μM sanguinarine for 12 hours, 24 hours, 48 hours, and 72 hours, using ELISA. (E,F) A7r5 and HMVEC cells were cultured with 30 ng/mL VEGF in media containing 2 μM sanguinarine and incubated for 24 hours. Cell viability was assessed using the CCK assay (E), and cell apoptosis was evaluated through PI/RNase A staining followed by flow cytometry (F). The ability of cells to migrate was assessed using a wound healing assay, with representative images displaying the scratch assay results (G). Scale bar = 20 μm. (H) The representative images from the tube formation assay were included. Scale bar = 20 μm. *$p < 0.05$, **$p < 0.01$, ***$p < 0.001$, ****$p < 0.0001$ compared to 0 μM; $^{\#}p < 0.05$, $^{\#\#}p < 0.01$ compared to the sanguinarine + VEGF treatment; ns, no significance.

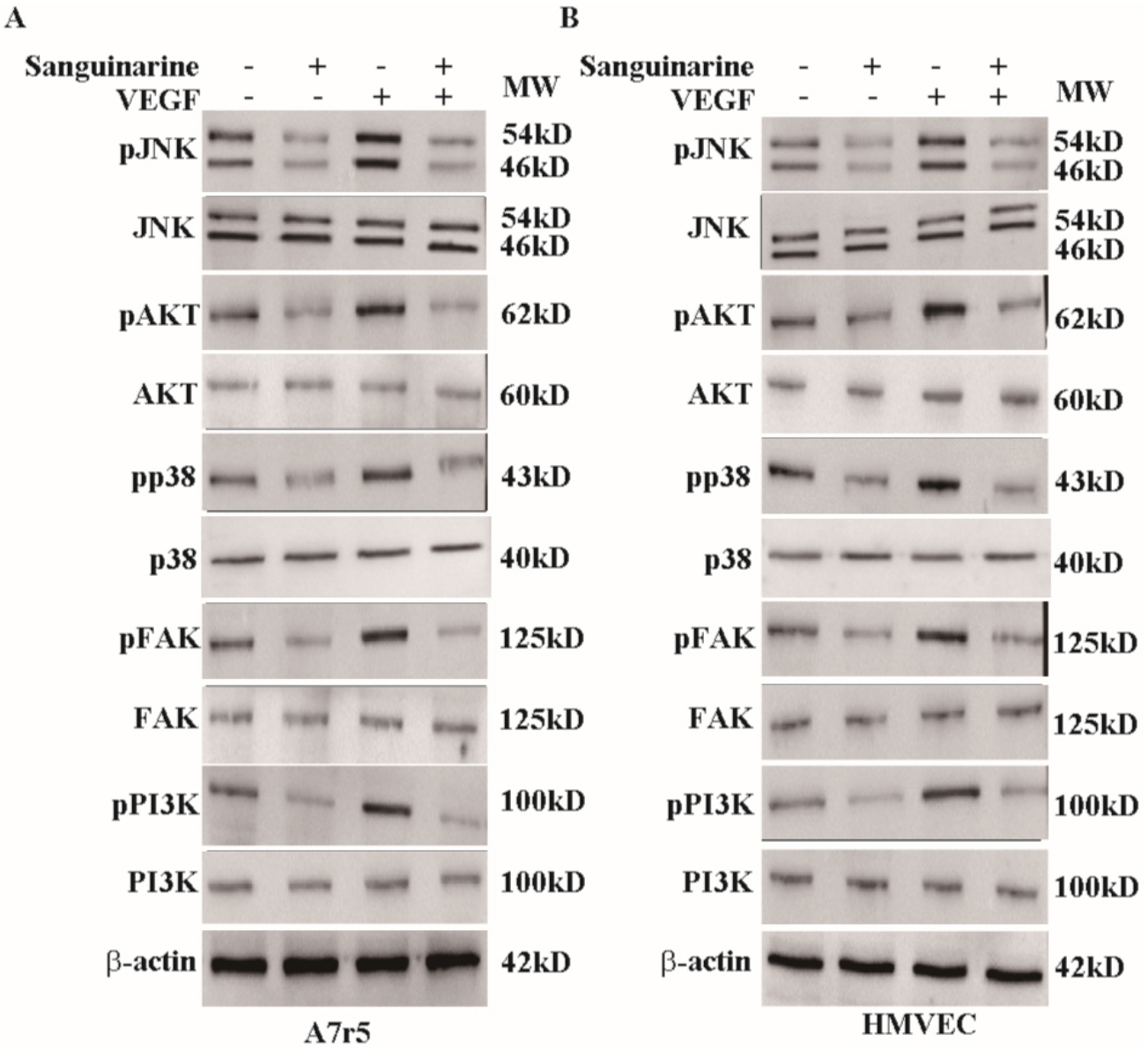

Fig. 5. Sanguinarine inhibited VEGF-mediated protein expression. (A,B) VEGF (30 ng/mL) was added to the cultures of sub-confluent A7r5 (A) and HMVEC (B) cells in medium containing 2 μM concentrations of sanguinarine and then cultured for 30 minutes. Cell lysates were detected by western blot assay with antibodies to JNK, pJNK, AKT, pAKT(Ser473), FAK, pFAK(Tyr397), p38, pp38(Tyr182), PI3K, pPI3K and β-actin. n = 3.

tion. Notably, there was a marked upregulation of cell cycle-regulated proteins p27 and E-cadherin. Moreover, sanguinarine substantially inhibited VEGF transcription, which in turn affected the VEGF signaling pathway. Our results indicate that the anti-angiogenic effects of sanguinarine are mediated by repressing VEGF signal transduction activation through the dephosphorylation of Akt (Ser473), p38 (Tyr182), and E-cadherin (Tyr658). Importantly, these effects appeared reversible, as significant or complete recovery was observed upon the addition of VEGF. Thus, the cell cycle arrest and migration inhibition induced by sanguinarine may be primarily mediated through the VEGF signaling pathway and its downstream effects.

Although other target proteins or mechanisms could also contribute to these processes, we hypothesize that the anti-angiogenic effect is largely driven by blocking the VEGF-induced downstream signaling pathway. It was reported that VEGF is a principal molecular driver of tumor angiogenesis, and inhibitors of the VEGF pathway are being explored as potential cancer treatments [19]. Additionally, Xu *et al.* [20] reported that sanguinarine reduces or blocks the phosphorylation activation of Akt, E-cadherin, and p38, all of which are modulators in the VEGF signaling pathway. This finding aligns with the results of the present study. However, the direct targeting of sanguinarine to VEGF remains unconfirmed, and further molecular dock-

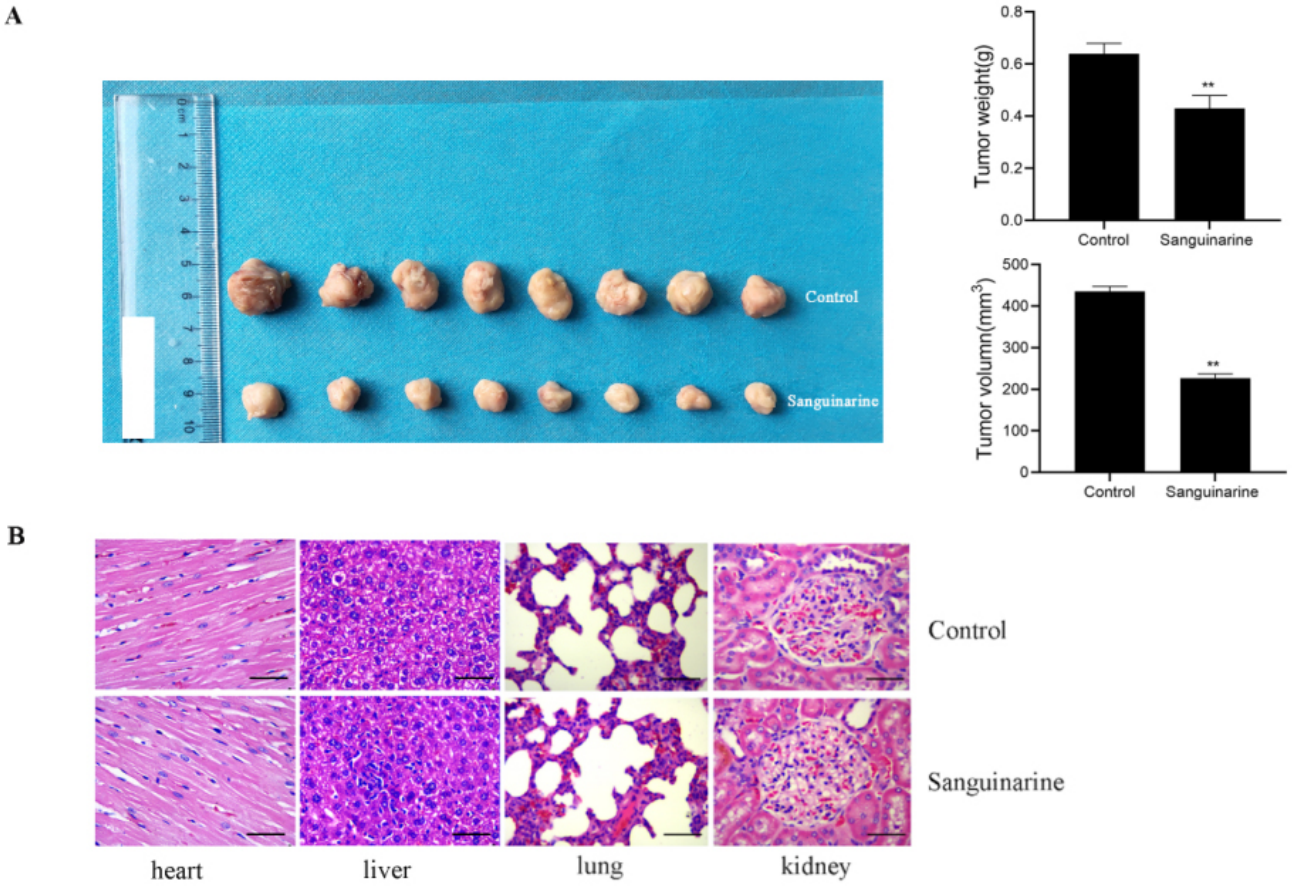

Fig. 6. Sanguinarine inhibited tumor growth and without toxicity characteristics. (A) Representative images of tumors and statistical analysis of volumes and weight. (B) Hematoxylin and eosin (HE) staining in tissues of the heart, liver, kidney, and lung (×400). Scale bar = 20 µm. n = 8. $^{**}p < 0.01$ vs Control.

ing analyses between sanguinarine and VEGF protein are warranted in future research. Vascular endothelial-cadherin is an endothelial cell-specific adhesion molecule that regulates angiogenesis [21]. Other studies have shown that E-cadherin contributes to endothelial cell migration, maintains vascular integrity, and supports the formation of tubular structures [22].

Furthermore, p27kip1 haploinsufficiency has been associated with improved cardiac function in the early stages of myocardial infarction and has been linked to enhanced angiogenesis [23].

Consistent with the above reports, sanguinarine represses p27 and E-cadherin expressions and significantly inhibits tube formation. Our previous studies revealed that Ras-related C3 botulinum toxin substrate 1b (*RAC1b*), a tumor-related *RAC1* (Rac Family Small GTPase 1) splice variant, was overexpressed and that its level was linked to poor clinical outcomes [24,25]. As a benzophenanthridine alkaloid, sanguinarine specifically inhibits the proliferation of tumor cells expressing *RAC1b* splice variants. Several beneficial properties of sanguinarine promote its antioxidant, antimicrobial, and anti-inflammatory effects [26]. Consistently, one researcher has demonstrated that sanguinarine impedes tumor metastasis and development by disrupting a wide range of cell signaling pathways and its molecular targets, such as B-cell lymphoma-2 (BCL-2), Mitogen-activated protein kinases (MAPKs), Protein Kinase B (Akt), Nuclear factor kappa-B (NF-κB), Reactive oxygen species (ROS), and microRNAs (miRNAs) [7], and sanguinarine has no negative effects on the health status of birds [27]. Furthermore, sanguinarine was reported to inhibit the viability of breast cancer cells by inducing apoptosis through the upregulation of p27, downregulation of cyclin D1, and inhibition of the activation of Signal transducer and activator of transcription 3 (STAT3) [28]. Sanguinarine accumulates in intracellular spaces at high concentrations, exhibiting cytotoxicity against cancer cell lines [29], which markedly improves cancer therapy. Our findings show that sanguinarine displays insignificant toxicity to healthy cells and tissues.

The anti-proliferative action of sanguinarine against cancer cells remains controversial in the targeted therapy field. Our work confirms the possibility that sanguinarine is an anti-angiogenic natural product that directly represses the pro-proliferative and migratory effects of VEGF on the endothelial cell line. Our findings indicate that sanguinar-

ine is a potentially novel VEGF inhibitor and provide valuable information for a better understanding of its anti-cancer properties.

Conclusion

In conclusion, sanguinarine is an anti-angiogenic natural product that may repress the pro-proliferative and migratory effects of VEGF on the endothelial cell line. Thus, this suggests that it harbors anticancer effects.

Availability of Data and Materials

The datasets used and/or analyzed during the current study are available from the corresponding author on reasonable request.

Author Contributions

The project was conceived and designed by WNW and LY. The experiments were conducted by LY, WL, SS, CSZ, YYZ, and XTZ. Data were analyzed by LY and WNW. The manuscript was written by WNW. All authors were involved in drafting the manuscript or revising it critically for important intellectual content. All authors read and approved the final manuscript. All authors have participated sufficiently in the work and agreed to be accountable for all aspects of the work.

Ethics Approval and Consent to Participate

All animal experiments were conducted in accordance with the guidelines of the Animal Ethics Committee of Medical Discovery Leader (MDL, Approval number: MDL2022-06-14-02) and followed the Guide for the Care and Use of Laboratory Animals published by the Chinese National Institutes of Health.

Acknowledgment

Not applicable.

Funding

This work was supported by the Scientific Research Project of Chongming District Science and Technology Commission. The program No. is CKY2022-22.

Conflict of Interest

The authors declare no conflict of interest.

Supplementary Material

Supplementary material associated with this article can be found, in the online version, at https://doi.org/10.24976/Discov.Med.202537200.173.

References

[1] Yanagisawa H, Sugimoto M, Miyashita T. Mathematical simulation of tumour angiogenesis: angiopoietin balance is a key factor in vessel growth and regression. Scientific Reports. 2021; 11: 419. https://doi.org/10.1038/s41598-020-79824-8.

[2] Liu ZL, Chen HH, Zheng LL, Sun LP, Shi L. Angiogenic signaling pathways and anti-angiogenic therapy for cancer. Signal Transduction and Targeted Therapy. 2023; 8: 198. https://doi.org/10.1038/s41392-023-01460-1.

[3] Lv S, Liu Y, Xie C, Xue C, Du S, Yao J. Emerging role of interactions between tumor angiogenesis and cancer stem cells. Journal of Controlled Release. 2023; 360: 468–481. https://doi.org/10.1016/j.jconrel.2023.06.036.

[4] Ye ZW, Yu ZL, Chen G, Jia J. Extracellular vesicles in tumor angiogenesis and resistance to anti-angiogenic therapy. Cancer Science. 2023; 114: 2739–2749. https://doi.org/10.1111/cas.15801.

[5] Caballero-George C, Vanderheyden PML, Apers S, Van den Heuvel H, Solis PN, Gupta MP, *et al*. Inhibitory activity on binding of specific ligands to the human angiotensin II AT(1) and endothelin 1 ET(A) receptors: bioactive benzo[c]phenanthridine alkaloids from the root of Bocconia frutescens. Planta Medica. 2002; 68: 770–775. https://doi.org/10.1055/s-2002-34406.

[6] Mackraj I, Govender T, Gathiram P. Sanguinarine. Cardiovascular Therapeutics. 2008; 26: 75–83. https://doi.org/10.1111/j.1527-3466.2007.00037.x.

[7] Ullah A, Ullah N, Nawaz T, Aziz T. Molecular Mechanisms of Sanguinarine in Cancer Prevention and Treatment. Anti-cancer Agents in Medicinal Chemistry. 2023; 23: 765–778. https://doi.org/10.2174/1871520622666220831124321.

[8] Ahmad N, Gupta S, Husain MM, Heiskanen KM, Mukhtar H. Differential antiproliferative and apoptotic response of sanguinarine for cancer cells versus normal cells. Clinical Cancer Research. 2000; 6: 1524–1528.

[9] Balestrini L, Di Donfrancesco A, Rossi L, Marracci S, Isolani ME, Bianucci AM, *et al*. The natural compound sanguinarine perturbs the regenerative capabilities of planarians. The International Journal of Developmental Biology. 2017; 61: 43–52. https://doi.org/10.1387/ijdb.160169rb.

[10] Byrne AM, Bouchier-Hayes DJ, Harmey JH. Angiogenic and cell survival functions of vascular endothelial growth factor (VEGF). Journal of Cellular and Molecular Medicine. 2005; 9: 777–794. https://doi.org/10.1111/j.1582-4934.2005.tb00379.x.

[11] Carmeliet P, Jain RK. Molecular mechanisms and clinical applications of angiogenesis. Nature. 2011; 473: 298–307. https://doi.org/10.1038/nature10144.

[12] Aggarwal C, Somaiah N, Simon G. Antiangiogenic agents in the management of non-small cell lung cancer: where do we stand now and where are we headed? Cancer Biology & Therapy. 2012; 13: 247–263. https://doi.org/10.4161/cbt.19594.

[13] Farhat FS, Tfayli A, Fakhruddin N, Mahfouz R, Otrock ZK, Alameddine RS, *et al*. Expression, prognostic and predictive impact of VEGF and bFGF in non-small cell lung cancer. Critical Reviews in Oncology/hematology. 2012; 84: 149–160. https://doi.org/10.1016/j.critrevonc.2012.02.012.

[14] Cui Y, Luo Y, Qian Q, Tian J, Fang Z, Wang X, *et al*. Sanguinarine Regulates Tumor-Associated Macrophages to Prevent Lung Cancer Angiogenesis Through the WNT/β-Catenin Pathway. Frontiers in Oncology. 2022; 12: 732860. https://doi.org/10.3389/fonc.2022.732860.

[15] Lou G, Wang J, Hu J, Gan Q, Peng C, Xiong H, *et al*. Sanguinarine: A Double-Edged Sword of Anticancer and Carcinogenesis and Its Future Application Prospect. Anti-cancer Agents in Medicinal Chemistry. 2021; 21: 2100–2110. https://doi.org/10.2174/1871520621666210126091512.

[16] Basini G, Santini SE, Bussolati S, Grasselli F. The plant alkaloid sanguinarine is a potential inhibitor of follicular angiogenesis. The Journal of Reproduction and Development. 2007; 53: 573–579. https://doi.org/10.1262/jrd.18126.

[17] Eun JP, Koh GY. Suppression of angiogenesis by the plant alkaloid, sanguinarine. Biochemical and Biophysical Research Communications. 2004; 317: 618–624. https://doi.org/10.1016/j.bbrc.2004.03.077.

[18] Zeng H, Dvorak HF, Mukhopadhyay D. Vascular permeability factor (VPF)/vascular endothelial growth factor (VEGF) peceptor-1 down-modulates VPF/VEGF receptor-2-mediated endothelial cell proliferation, but not migration, through phosphatidylinositol 3-kinase-dependent pathways. The Journal of Biological Chemistry. 2001; 276: 26969–26979. https://doi.org/10.1074/jbc.M103213200.

[19] Li Y, Li H, Wei X. Long noncoding RNA LINC00261 suppresses prostate cancer tumorigenesis through upregulation of GATA6-mediated DKK3. Cancer Cell International. 2020; 20: 474. https://doi.org/10.1186/s12935-020-01484-5.

[20] Xu JY, Meng QH, Chong Y, Jiao Y, Zhao L, Rosen EM, *et al*. Sanguinarine is a novel VEGF inhibitor involved in the suppression of angiogenesis and cell migration. Molecular and Clinical Oncology. 2013; 1: 331–336. https://doi.org/10.3892/mco.2012.41.

[21] Giannotta M, Trani M, Dejana E. VE-cadherin and endothelial adherens junctions: active guardians of vascular integrity. Developmental Cell. 2013; 26: 441–454. https://doi.org/10.1016/j.devcel.2013.08.020.

[22] Wong SHM, Fang CM, Chuah LH, Leong CO, Ngai SC. E-cadherin: Its dysregulation in carcinogenesis and clinical implications. Critical Reviews in Oncology/hematology. 2018; 121: 11–22. https://doi.org/10.1016/j.critrevonc.2017.11.010.

[23] Zhou N, Fu Y, Wang Y, Chen P, Meng H, Guo S, *et al*. p27 kip1 haplo-insufficiency improves cardiac function in early-stages of myocardial infarction by protecting myocardium and increasing angiogenesis by promoting IKK activation. Scientific Reports. 2014; 4: 5978. https://doi.org/10.1038/srep05978.

[24] Ying L, Li G, Wei SS, Wang H, An P, Wang X, *et al*. Sanguinarine inhibits Rac1b-rendered cell survival enhancement by promoting apoptosis and blocking proliferation. Acta Pharmacologica Sinica. 2015; 36: 229–240. https://doi.org/10.1038/aps.2014.115.

[25] Li G, Ying L, Wang H, Wei SS, Chen J, Chen YH, *et al*. Rac1b enhances cell survival through activation of the JNK2/c-JUN/Cyclin-D1 and AKT2/MCL1 pathways. Oncotarget. 2016; 7: 17970–17985. https://doi.org/10.18632/oncotarget.7602.

[26] Gupta SC, Kim JH, Prasad S, Aggarwal BB. Regulation of survival, proliferation, invasion, angiogenesis, and metastasis of tumor cells through modulation of inflammatory pathways by nutraceuticals. Cancer Metastasis Reviews. 2010; 29: 405–434. https://doi.org/10.1007/s10555-010-9235-2.

[27] Manaa EA, Abdel-Latif MA, Ibraheim SE, Sakr A, Dawood M, Albadrani GM, *et al*. Impacts of *Macleaya cordata* on Productive Performance, Expression of Growth-Related Genes, Hematological, and Biochemical Parameters in Turkey. Frontiers in Veterinary Science. 2022; 9: 873951. https://doi.org/10.3389/fvets.2022.873951.

[28] Malla RR, Bhamidipati P, Adem M. Insights into the potential of Sanguinarine as a promising therapeutic option for breast cancer. Biochemical Pharmacology. 2023; 212: 115565. https://doi.org/10.1016/j.bcp.2023.115565.

[29] Vogel M, Lawson M, Sippl W, Conrad U, Roos W. Structure and mechanism of sanguinarine reductase, an enzyme of alkaloid detoxification. The Journal of Biological Chemistry. 2010; 285: 18397–18406. https://doi.org/10.1074/jbc.M109.088989.